Molecular Biology of the Cell
Vol. 17, 3446–3455, August 2006

A Role for the Mitogen-activated Protein Kinase Kinase Kinase 1 in Epithelial Wound Healing[D]

Maoxian Deng,*† Wei-Li Chen,†‡§ Atsushi Takatori,* Zhimin Peng,* Lin Zhang,*‖ Maureen Mongan,* Ranjani Parthasarathy,* Maureen Sartor,* Marian Miller,* Jianhua Yang,¶ Bing Su,¶ Winston W.-Y. Kao,§ and Ying Xia*§

*Departments of Environmental Health and Center for Environmental Genetics, University of Cincinnati Medical Center, Cincinnati, OH 45267-0056; ‡Department of Ophthalmology, National Taiwan University Hospital, Taipei, Taiwan, Republic of China; §Department of Ophthalmology, University of Cincinnati Medical Center, Cincinnati, OH 45267; ‖Department of Central Lab, Southern Medical University, Tonghe, Guangzhou, People's Republic of China; and ¶Department of Immunology, M. D. Anderson Cancer Center, University of Texas, Houston, TX 77030

Submitted February 6, 2006; Revised May 15, 2006; Accepted May 25, 2006
Monitoring Editor: J. Silvio Gutkind

The mitogen-activated protein kinase kinase (MEK) kinase 1 (MEKK1) mediates activin B signals required for eyelid epithelium morphogenesis during mouse fetal development. The present study investigates the role of MEKK1 in epithelial wound healing, another activin-regulated biological process. In a skin wound model, injury markedly stimulates MEKK1 expression and activity, which are in turn required for the expression of genes involved in extracellular matrix (ECM) homeostasis. MEKK1 ablation or down-regulation by interfering RNA significantly delays skin wound closure and impairs activation of Jun NH_2-terminal kinases, induction of plasminogen activator inhibitor (PAI)-1, and restoration of cell–cell junctions of the wounded epidermis. Conversely, expression of wild-type MEKK1 accelerates reepithelialization of full-thickness skin and corneal debridement wounds by mechanisms involving epithelial cell migration, a cell function that is partially abolished by neutralizing antibodies for PAI-1 and metalloproteinase III. Our data suggest that MEKK1 transmits wound signals, leading to the transcriptional activation of genes involved in ECM homeostasis, epithelial cell migration, and wound reepithelialization.

INTRODUCTION

Tissue injury initiates a cascade of events, including inflammation, new tissue formation, and tissue remodeling, to reconstruct the wounded area. Remodeling is triggered by growth factors and cytokines, which stimulate the migration and proliferation of keratinocytes at the wound edge. These cells migrate on the injury-induced provisional extracellular matrices, eventually completing reepithelialization to form a neoepidermis that covers the wound (Werner and Grose, 2003). One growth factor critical for reepithelialization is activin B, a member of the transforming growth factor-β family, that signals through binding to the specific cell surface receptor ACTR. Skin injury induces a marked elevation of activin B expression in the hyperproliferative epithelium at the wound edge and in the migrating epithelial tongue (Hubner *et al*., 1996), while blocking activin B activity by overexpression of a dominant negative ACTR mutant in skin keratinocytes or of follistatin, a soluble activin antagonist, significantly delays wound reepithelialization (Wankell *et al*., 2001; Bamberger *et al*., 2005). Activin B can activate the Smad2/Smad3/Smad4 transcription complexes to control gene expression and cell function; however, its role in wound healing is propagated through Smad3-independent mechanisms, because Smad3 ablation accelerates skin wound closure instead of slowing it down (Ashcroft *et al*., 1999).

Activin B also has a role in the regulation of mouse fetal eyelid development via a signal transduction pathway involving mitogen-activated protein kinase kinase kinase (MEKK)1, a mitogen-activated protein kinase (MAPK) kinase kinase known to control specific MAPK activation (Schlesinger *et al*., 1998). The activin B–MEKK1 pathway leads to the activation of the Jun NH_2-terminal kinase (JNK) MAPK and epithelial cell migration. This results in the movement of the embryonic eyelid epithelium to the center of the eye and the developmental eyelid fusion (Zhang *et al*., 2003). *Activin βB* knockout mice, follistatin transgenic mice, and *Mekk1* knockout mice all suffer from failure of embryonic eyelid closure and exhibit an "eye-open" at birth phenotype (Feijen *et al*., 1994; Vassalli *et al*., 1994; Schrewe *et al*., 1994; Yujiri *et al*., 2000; Zhang *et al*., 2003). The biological process of embryonic eyelid closure is in fact quite similar to that of wound reepithelialization, both involving epithelial cell migration over extracellular matrices (ECMs). This sim-

This article was published online ahead of print in *MBC in Press* (http://www.molbiolcell.org/cgi/doi/10.1091/mbc.E06–02–0102) on June 7, 2006.

[D] The online version of this article contains supplemental material at *MBC Online* (http://www.molbiolcell.org).

† These authors contributed equally to this work.

Address correspondence to: Ying Xia (xiay@email.uc.edu).

Abbreviations used: ECM, extracellular matrix; iRNA, interfering RNA; JNK, Jun NH_2-terminal kinase; MAPK, mitogen-activated protein kinase; MEKK, mitogen-activated protein kinase kinase kinase; PAI, plasminogen activator inhibitor.

Table 1. Activin B-induced and MEKK1-dependent genes

Classification	Clone	Name	Symbol	C wt:ko	A wt:ko	Ko A:C	wt A:C
Cell migration	M33960	Serine (or cysteine) proteinase inhibitor, Clade E, 1	Pai-1	1.77[a]	21.05	1.06	12.54
	V00755	Tissue inhibitor of metalloproteinase 1	Timp1	1.92	6.20	−1.01	3.18
	X15591	Cytotoxic T lymphocyte-associated protein 2α	Ctla2a	4.98	12.30	1.05	2.58
	X63162	Matrix metalloproteinase 3	Mmp3	2.57	5.10	1.09	2.16
	AP053368	Lysyl oxidase-like 3	Loxl3	2.51	4.34	1.25	2.15
	NM_007969	Extracellular proteinase inhibitor	Expi	2.36	5.61	−1.23	1.94
	AB006458	Mannosidase 2α B2	Man2b2	2.04	3.62	1.09	1.94
ECM	NM_011607	Tenascin C	Tnc	2.14	7.05	−1.14	2.88
	M87276	Thrombospoindin 1	Thbs1	1.79	3.6	1.10	2.23
	X52046	Procollagen, type III, α1	Col3a1	2.83	5.97	−1.04	2.02
	J04694	Procollagen, type IV, α1	Col4a1	2.25	4.07	1.05	1.90
Signaling	AB020886	A kinase (PRKA) anchor protein (gravin) 12	Gravin12	2.09	6.54	−1.00	3.12
Oxidative stress	U62658	Glutathione peroxidase	Gpx2	3.61	7.42	−1.21	1.70

A, activin B; C, control; ko, keratinocytes from MEKK1-deficient mice; and wt, keratinocytes from wild-type mice.
[a] The numbers represent -fold differences.

ilarity led us to hypothesize that the developmental activin–MEKK1 pathway is reactivated during tissue injury and that MEKK1 transduces signals required for wound reepithelialization and closure.

In this article, we test this hypothesis and describe a role for MEKK1 in injury repair. We show that MEKK1 is expressed in skin epithelial cells and that its expression and activity are elevated by skin injury. MEKK1 ablation in mice reduces JNK phosphorylation and skin wound closure, whereas MEKK1 overexpression promotes the closure of corneal and skin wounds. In skin keratinocytes, MEKK1 is essential for activin B to stimulate, among other extracellular matrices and matrix remodeling enzymes, the plasminogen activator inhibitor 1 (*Pai-1*), whose expression in skin wounds is markedly reduced by MEKK1 ablation and enhanced by MEKK1 overexpression.

MATERIALS AND METHODS

Reagents, Antibodies, and Mouse Colonies

Mouse epidermal keratinocytes were prepared from newborn pups, as described previously (Rouabhia *et al.*, 1992). The keratinocyte growth media (KGM) were from Cascade Biology (Portland, OR), and all other cell culture reagents were from Invitrogen (Carlsbad, CA). The chemical inhibitors metalloproteinase III (MMP-3) inhibitor VIII, SP600125, PD98059, and SB202190 were from Calbiochem (San Diego, CA). Antibodies for detecting PAI-1 by immunohistochemistry were from America Diagnostica (Stamford, CT) and for neutralizing PAI-1 were from Calbiochem. Anti-MEKK1 was described previously (Xia *et al.*, 1998). The *Mekk1*$^{\Delta KD/\Delta KD}$ and *Mekk1*$^{\Delta KD/\Delta KD}$ mice were described previously (Zhang *et al.*, 2003), and the wild-type C57/BL6 mice were purchased from The Jackson Laboratory (Bar Harbor, ME). All experiments conducted with these animals have been approved by the University of Cincinnati Animal Care and Use Committee.

Adenovirus (Ad) Preparation and Infection

A 4.9-kb DNA fragment containing the cDNA for human wild-type MEKK1 {MEKK1(WT)} or the kinase-inactive mutant {MEKK1(KM)} (Xia *et al.*, 1998) was cloned in the pShuttle-cytomegalovirus (CMV) vector (Stratagene, La Jolla, CA). To generate Ad MEKK1 small interfering RNA (siRNA), first, the CMV promoter in pAdtrack vector was replaced by a U6 promoter using standard molecular cloning techniques. Second, a double-strand DNA fragment containing a complementary human *MEKK1*, nucleotides 2819–2837 (italics), encompassing a hairpin loop (lowercase) and a poly T tail (*ACAAAAGGCAGACCCCACA*ttcaagaga*TGTGGGGTCTGCCTTTTGT*TTTTTTTG-GAA) was cloned into the HindIII sites downstream of U6 promoter of pAdtrack-U6 vector. Recombination with pAdEasy-1 vector, viral DNA purification, transfection of Ad 293 cells, and adenovirus preparation and titration were all performed following the manufacturer's instructions (Stratagene). The Ad green fluorescent protein (GFP) was originated from pAdtrack, the Ad β-galactosidase (β-Gal) was provided by the manufacturer, and the Ad MKK6 and Ad MKK7 were as described previously (Zhang *et al.*, 2005).

In Vivo and In Vitro Wound Healing Assay

Ten-week-old wild-type (C57/BL6) and *Mekk1*$^{\Delta KD/\Delta KD}$ mice were shaved and deeply anesthetized by intraperitoneal 2,2,2-tribromoethanol (avertin) (100 μg/g body weight) injection. Four full-thickness skin wounds of 0.5 × 0.5 cm were made on each mouse at the dorsal skin with sterile scissors. To some wounds, a total of 2×10^7 plaque-forming units (PFU) of adenoviruses were injected intradermally around the wound edges. Wounds were left uncovered, and the wound areas were measured at various daily intervals after injury. The complete wounds with 4-mm margins were isolated and the tissues were fixed for histological analysis or were subjected to protein isolation.

For in vivo corneal wounding, 10-wk-old C57/BL6 mice were anesthetized by intraperitoneal injection of combined xylazine (13 mg/kg) and ketamine (87 mg/kg) and topical oxybuprocaine (Santen, Osaka, Japan). A central corneal epithelial debridement (2 mm in diameter) was created using an Algerbrush IITM corneal rust ring remover with a 0.5-mm burr (Alger Equipment, Lago Vista, TX). The remaining corneal wound area was determined by fluorescein staining, observed under a stereomicroscope (Stems SV11; Carl Zeiss, Thornwood, NY) and measured by the computer image analysis system Scion Image Beta 4.02 (available at http://www.scioncorp.com). All animals were given intraperitoneal injection of 5-bromo-2′-deoxyuridine (BrdU) (400 μg/kg) (Sigma-Aldrich, St. Louis, MO) 4 h before being killed.

For ex vivo organ culture, 10-wk-old C57/BL6 mice were killed by CO_2 asphyxiation, and the eyes were isolated. An epithelial defect of 2 mm in diameter was created as described above, and the individually enucleated eyes were cultured in 1.0 ml of DMEM supplemented with 1.4% fetal bovine serum (FBS) with or without the presence of MAPK inhibitors. Some eyes were subjected to incubation with 10^7 PFU/ml adenoviruses for 1 h before culturing. At 34 h of culturing, 40 μg/ml BrdU (Sigma-Aldrich) was added in the culture medium for 2 h. Healing of the epithelial defect was determined by the method described above for the in vivo study.

For in vitro wound healing assays, 80% confluent monolayers of wild-type epidermal keratinocytes, dermal fibroblasts, or human HaCaT cells were incubated with adenoviruses at the indicated PFU/cell for 1 h. The infected cells were subjected to starvation in the absence of growth factors and FBS for 24 h, before scratch wounds were created on the cell surface with a micropipette tip. The wound healing was carried out for 16–24 h in growth factor-free medium and was photographed at various times after wounding. To some samples, MAPK inhibitors (5 μM) were added after adenoviral infection. The MMP-3 inhibitors (10 μM) and PAI-1 neutralizing antibody (5 μg/ml) were added to the media 4 h before the scratch wounding.

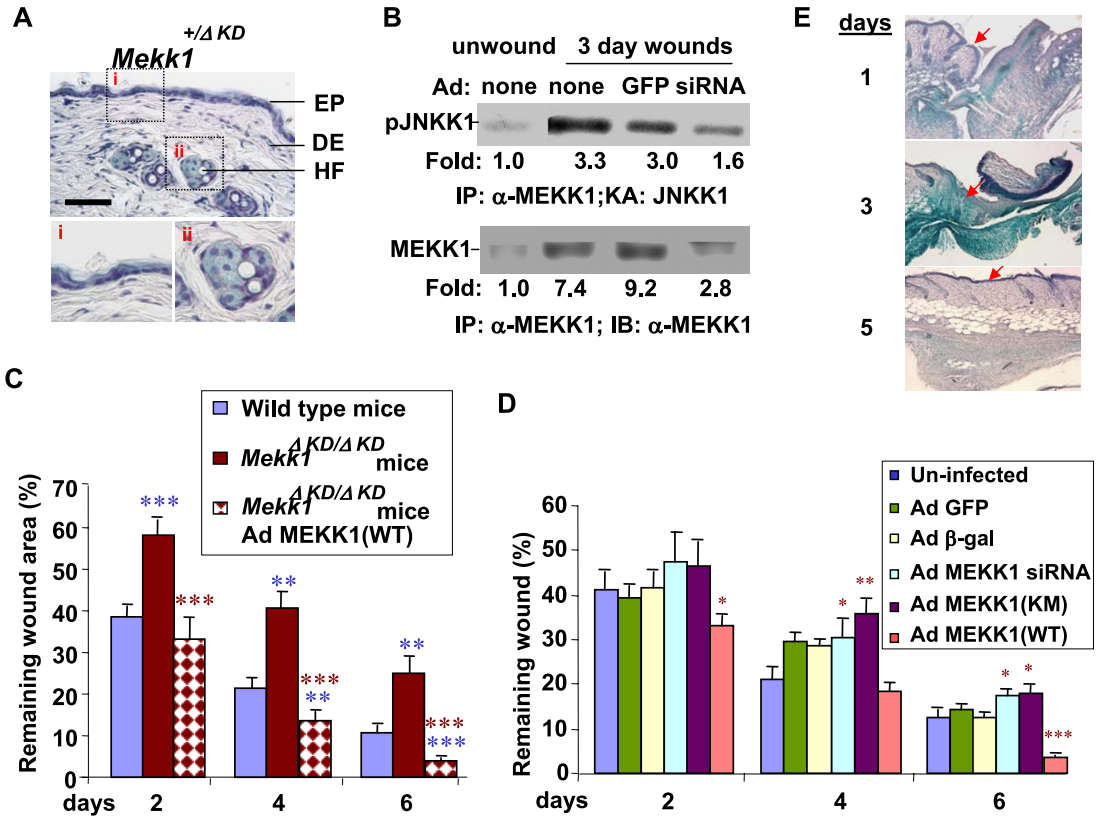

Figure 1. MEKK1 is required for optimal skin wound closure. (A) Skin from *Mekk1*$^{+/\Delta KD}$ mice was stained with X-Gal. Tissue sections were examined for blue X-Gal–positive cells accumulating in the epidermis (i) and hair follicles (ii), as indicated. DE, dermis; EP, epithelium; HF, hair follicles. Bar, 50 μm. (B) Wounds on wild-type mice were either uninfected or infected by adenoviruses for GFP and MEKK1 siRNA. Protein lysates from normal and day 3-wounded skin tissues were subjected to immunoprecipitation using α-MEKK1, followed by an in vitro kinase assay using GST-JNKK1 as a substrate (top) and Western blotting using α-MEKK1 (bottom). The -fold induction of MEKK1 expression and kinase activity were relative to those in unwounded skin tissues. (C) Full-thickness excision wounds were created on the dorsal side of wild-type and *Mekk1*$^{\Delta KD/\Delta KD}$ mice. The *Mekk1*$^{\Delta KD/\Delta KD}$ wounds were either uninfected or infected with Ad MEKK1(WT). (D) Wounds on wild-type mice were either uninfected or subjected to infection by adenoviruses for β-Gal, MEKK1(WT), MEKK1(KM), GFP and MEKK1 siRNA. Wound areas were measured after various days of injury and are presented relative to the original wound size. The results represent the mean ± SD of at least 16 wounds of each condition. The means of the remaining wound area of each group were analyzed by the Student's *t* test. ***p $<$ 0.001, **p $<$ 0.01, and *p $<$ 0.05 are considered statistically significant. Comparisons of wounds between wild-type versus *Mekk1*$^{\Delta KD/\Delta KD}$ are labeled in blue; uninfected versus Ad-infected mice of the same genotype are labeled in red. (E) Adenoviruses for β-Gal were injected to the full-thickness skin wounds of wild-type mice. The wound tissues were isolated at various days after injury and subjected to X-Gal staining. Sections of the stained tissues were counterstained by hematoxylin and photographed and the blue β-Gal–positive cells could be identified in the wound tissues. Arrows point at the epidermis.

Histological Analyses, Immunohistochemistry, and 5-Bromo-4-chloro-3-indolyl-β-D-galactoside (X-Gal) Staining

Skin and corneas were fixed in 4% paraformaldehyde, dehydrated, and embedded in paraffin. Five micrometer-thick sections were deparaffinized, before staining with hematoxylin and eosin according to standard procedures. The wound tissues isolated from mice at day 3 of injury were subjected to immunohistochemistry as described previously (Liu *et al*., 1993), using anti-pJNK, pp38 and pERK at 1:100. The wounds isolated at days 1, 3, 5, and 7 were examined for PAI-1 expression by immunohistochemistry using anti-PAI-1 (1:500). Whole mount X-Gal staining of unwounded or wounded skins and corneas was performed as described previously (Henkemeyer *et al*., 1996). The stained tissues were processed for embedding and sectioning. After counterstaining with hematoxylin, the tissues were photographed using an Olympus DF plan microscope.

For electron microscopy, excised wound areas were flattened and immediately fixed by overnight immersion in 2% paraformaldehyde/2.5% glutaraldehyde in phosphate buffer, pH 7.3. Tissues were dehydrated, passed through propylene oxide, and embedded in Spurr's resin so that sections could be made perpendicular to the plane of the basement membrane. Thin sections were taken from wound edge areas, placed on naked copper grids, stained with lead citrate and uranyl acetate, and examined with transmission electron microscopy.

Cell Growth, Cell and Tissue Lysates, and Western Blot Analyses

Procedures for primary keratinocyte growth, adenoviral infection, and MAPK inhibitor treatment were as described for the in vitro wound healing assay. Twenty-four hours after infection and before harvesting, keratinocytes were maintained in growth factor-free KGM and fibroblasts in FBS-free DMEM, for 24 h. Under this condition, some cells were exposed to 5 ng/ml activin B for various times before harvesting, and cell lysates were prepared as described previously (Hibi *et al*., 1993).

Proteins were extracted from the normal and wound tissues as described previously (Chen *et al*., 2001b). Briefly, skin samples were cut into small pieces, placed on ice, and incubated in 500 μl of SDS lysis buffer {62.5 mM Tris-HCl, pH 6.8, 2% SDS, 10% glycerol, and 50 mM dithiothreitol} for 1 h. The lysates were sonicated four times, 5 s each, and centrifuged at 14,000 rpm at 4°C for 10 min. The supernatant fraction was diluted with 3 volumes of acetone and left on ice for 10 min. The suspension was centrifuged at 14,000 rpm at 4°C for 10 min, and the pellet was resuspended in 800 μl of acetone and centrifuged at 14,000 rpm at 4°C for 10 min. The pellet was then dissolved in 200 μl of SDS lysis buffer. The protein concentration was measured using the Bradford method (Bio-Rad, Hercules, CA). One hundred micrograms of lysate was subjected to SDS-PAGE, followed by transferring onto nitrocellulose membrane and probing with specific antibodies. Anti-PAI-1 was used at 1:500, anti-actin at 1:5000, and anti-MEKK1 at 1:200.

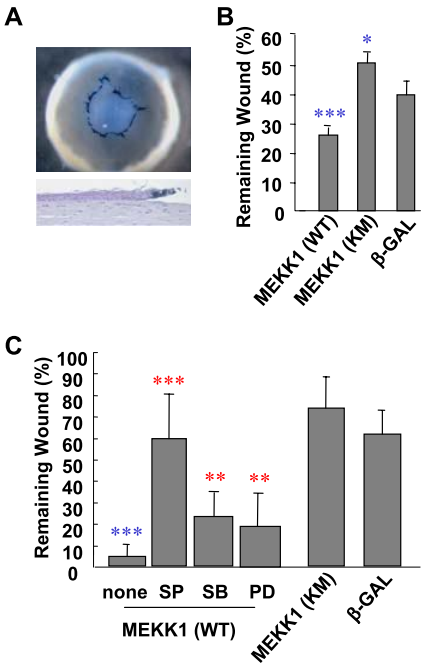

Figure 2. The MEKK1–JNK pathway stimulates corneal reepithelialization and wound healing. (A) β-Gal adenoviruses were applied as eyedrops to the corneal debridement wounds in mice. At 24 h after injury, the eye tissues were subjected to whole mount X-Gal staining (top). The stained tissues were sectioned and counterstained by hematoxylin (bottom) and the blue β-Gal–positive cells could be easily identified in the wounding edge epithelium. (B) Adenoviruses for β-Gal, MEKK1(WT), and MEKK1(KM) were used to infect corneal debridement wounds created in vivo on mouse eyes. The wound areas were measured at 24 h after injury and were calculated relative to the original wounds. Remaining wound areas were compared with those in Ad β-Gal–infected samples. (C) Corneal debridement wounds created on eyes maintained in ex vivo organ culture system were exposed to adenoviruses as indicated, in the presence or absence of MAPK inhibitors SP600125 (SP), SB202190 (SB), and PD98059 (PD) in the culture media. The wound areas were measured 36 h post injury and were calculated relative to the original wounds, or, in the case when inhibitors were used, relative to the wounds the absence of inhibitors. All data represent mean ± SD of at least eight wounds, and statistical analyses were carried out by Student's *t* test. The p values of ***$p < 0.001$, **$p < 0.01$, and *$p < 0.05$ are considered significantly different from the wounds of Ad β-Gal–infected eyes (in blue) or from the same Ad-infected wounds in the absence of the inhibitors (in red).

Immunoprecipitation and Immunocomplex Kinase Assay

Immunoprecipitation and in vitro kinase assay were done as described previously (Hibi *et al.*, 1993). In brief, 500 μg of tissue lysates was immunoprecipitated by anti-MEKK1 and protein A-agarose beads. The precipitates were either applied directly onto SDS-PAGE or subjected to in vitro kinase assays in the presence of [γ-^{32}P]ATP and 0.5 μg of glutathione *S*-transferase (GST)-JNK kinase 1 (JNKK1) as a substrate. The reactions were then loaded onto SDS-PAGE. After drying, the gel was exposed to x-ray film.

RNA Isolation, Fluorescent Labeling of Target cDNAs and High-Density Microarray Hybridization and Quantitative PCR (QPCR)

Wild-type and *Mekk1*$^{\Delta KD/\Delta KD}$ primary mouse keratinocytes were starved and treated with activin B for 12 h as described above. Total RNA was isolated using RNeasy kit (QIAGEN, Valencia, CA) according to the manufacturer's instructions. To verify RNA quality before labeling for microarray analyses, samples were analyzed using an Agilent 2100 Bioanalyzer (Agilent Technologies, Palo Alto, CA). cDNA was synthesized by reverse transcription of 20 μg of total RNA in a total volume of 30 μl containing 1× reverse transcriptase buffer, 2.5 μM random hexamers, 0.25 mM dNTP, 0.01 M dithiothreitol, 20 U of RNasin, and 200 U of SuperScript II RNase H$^-$ reverse transcriptase (Invitrogen). Samples were incubated at 42°C for 1 h, and the reverse transcriptase was inactivated by heating to 99°C for 5 min. Labeling of cDNAs, preparation of microarrays, and hybridization reactions were performed by the University of Cincinnati Functional Genomics Core (Cincinnati, OH), and specific details of the labeling protocols can be found at http://microarray.uc.edu. The statistical analyses are performed by the University of Cincinnati Bioinformatics Core, and detailed methods can be found in Supplemental Material.

QPCR analysis using SYBR Green (Invitrogen) and the designed primers was carried out to confirm microarray results. The reactions using Taq DNA Polymerase kit were performed according to the protocol provided by BD Biosciences (San Jose, CA), followed by detection by DNA Engine Opticon 2 real-time PCR detection system (MJ Research, Watertown, MA). Oligonucleotide primers were designed for glyceraldehyde 3-phosphate dehydrogenase (*Gapdh*), plasminogen activator inhibitor-1 (*Pai-1*), procollagen 3a1(*Procol 3a1*), thrombospondin-1(*thpbs-1*), and metalloprotease III (*Mmp-3*), The average cycle threshold value (CT) of *Gapdh* measurements in a PCR experiment was used to normalize the tested genes. The average CT values were determined by carrying out at least triplicate QPCR measurements for each gene in each experimental condition.

Data Normalization and Statistical Analyses

Microarray hybridization data representing raw spot intensities generated by the GenePix software were analyzed to identify differentially expressed genes under different experimental conditions. Data normalization was performed in three steps for each microarray separately. First, channel specific local background intensities were subtracted from the median intensity of each channel (Cy3 and Cy5). Second, background adjusted intensities were log-transformed, and the differences (R) and averages (A) of log-transformed values were calculated as $R = \log_2(X1) - \log_2(X2)$ and $A = [\log_2(X1) + \log_2(X2)]/2$, where X1 and X2 denote the Cy5 and Cy3 intensities after subtracting local backgrounds, respectively. Third, data centering was performed by fitting the array-specific local regression model of R as a function of A (Dudoit and Fridlyand, 2002). The difference between the observed log-ratio and the corresponding fitted value represented the normalized log-transformed gene expression ratio. Normalized log-intensities for the two channels were then calculated by adding half of the normalized ratio to A for the Cy5 channel and subtracting half of the normalized ratio from A for the Cy3 channel.

The statistical analysis was performed for each gene separately by fitting the following mixed effects linear model (Wolfinger *et al.*, 2001): $Y_{ijk} = \mu + A_i + S_j + C_k + \Omega_{ijk}$, where Y_{ijk} corresponds to the normalized log-intensity on the ith array (i = 1, . . . , 12), with the jth treatment combination (j = 1, . . . , 4), and labeled with the kth dye (k = 1 for Cy5, and 2 for Cy3). μ is the overall mean log-intensity, A_i is the effect of the ith array, S_j is the effect of the jth treatment combination, and C_k is the effect of the kth dye. Assumptions about model parameters were the same as described elsewhere (Wolfinger *et al.*, 2001), with array effects assumed to be random, and treatment and dye effects assumed to be fixed. Statistical significance of the differential expression between different treatment combinations, after adjusting for the array and dye effects, was assessed by calculating p values for corresponding linear contrasts. Multiple hypothesis testing adjustment was performed by calculating false discovery rate (FDR) values (Reiner *et al.*, 2003). Cut-off for significantly deregulated genes was set at a ratio of 2 above control values, and, for all the genes presented in Table 1, the FDR was <0.1 and the intensity was >200. Data normalization and statistical analyses were performed using SAS statistical software package (SAS Institute, Cary, NC).

RESULTS

MEKK1 Is Required for Optimal Skin Wound Closure

We detected strong MEKK1 expression in mouse skin epidermis and hair follicles, as demonstrated by the expression of an MEKK1 promoter-driven β-Gal fusion protein in the *Mekk1*$^{\Delta KD/\Delta KD}$ mice (Xia *et al.*, 2000; Figure 1A). Furthermore, a full-thickness skin injury markedly stimulated MEKK1 expression and activity (Figure 1B).

The induction of MEKK1 could in turn contribute to the healing process. To test this hypothesis, we examined the healing rate of full-thickness skin wounds in wild-type and *Mekk1*$^{\Delta KD/\Delta KD}$ mice. Although wounds in the two mice strains were indistinguishable on the basis of epithelium morphology and expression of markers for proliferating (keratin 6) or suprabasal (keratin 10) epithelial cells (Supplemental Figure S1A), wound closure rate was much reduced in the *Mekk1*$^{\Delta KD/\Delta KD}$ mice (Figure 1C). Reconstituting MEKK1 expression in the *Mekk1*$^{\Delta KD/\Delta KD}$ wounds with ade-

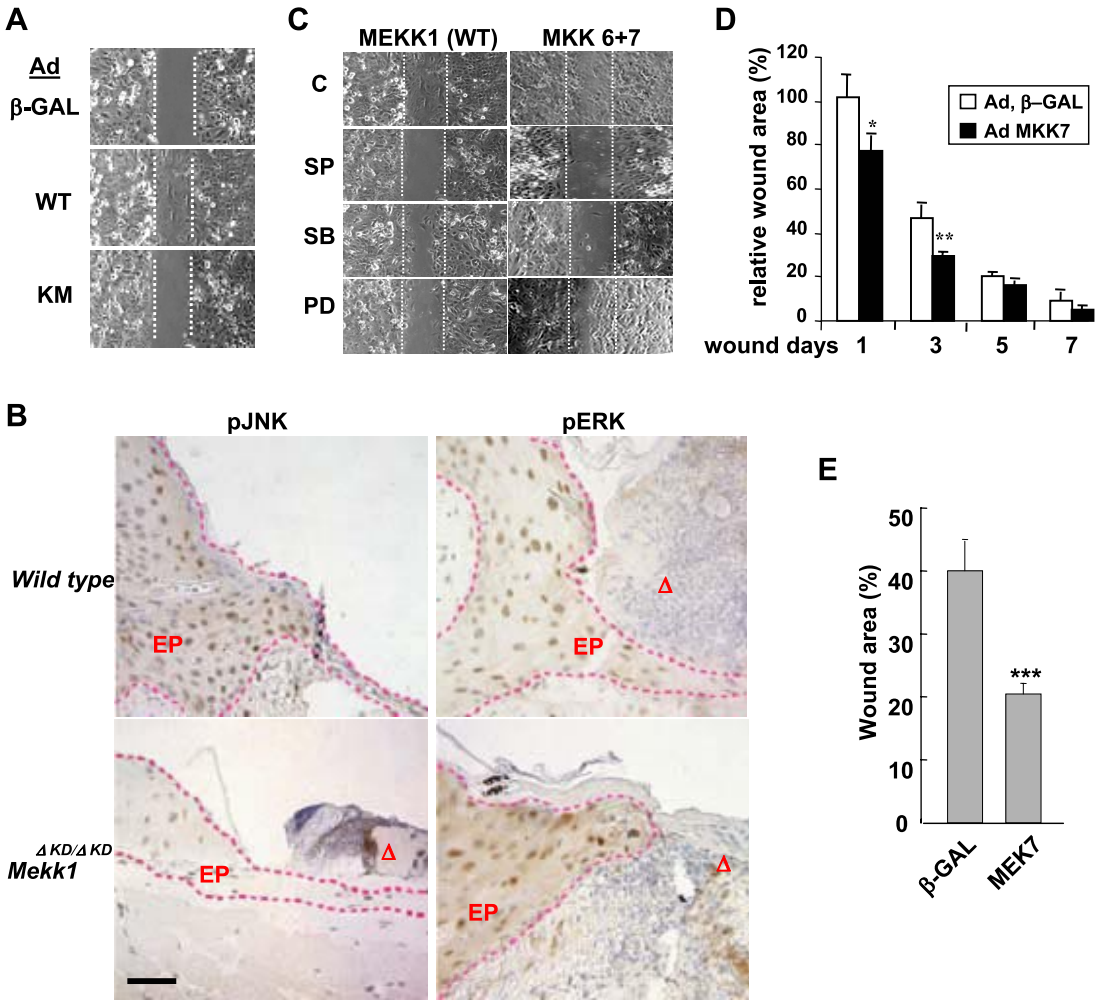

Figure 3. Activation of MEKK1 and JNK is sufficient for keratinocyte migration and skin wound closure. (A) Epidermal keratinocytes were infected by adenoviruses as indicated. The cells were subjected to in vitro wound healing assays and were photographed at 24 h after injury. (B) Skin wound tissues at day 3 after injury were subjected to immunohistochemistry staining for phosphorylated JNK (pJNK) and ERK (pERK), and the positive (brown color) staining was evident in the epidermis of wild-type mice. The epithelium in the wounds is marked by red dotted lines, and pJNK-positive cells were markedly reduced in the epithelium of *Mekk1*$^{\Delta KD/\Delta KD}$ mice. EP, epithelium and the triangle (Δ) indicates wound exudates. Bar, 50 μm. (C) Cells infected with Ad MEKK1(WT), and Ad MKK6 and Ad MKK7, as indicated, were subjected to in vitro wound healing assays in the absence and presence of various MAPK inhibitors and photographed at 24 h after injury. (D) Full-thickness skin wounds were generated on the dorsal side of wild-type mice. The wounds were exposed to adenoviruses for β-Gal and MKK7. Wound areas were measured at various days after injury, as indicated. (E) Corneal debridement wounds created on eyes maintained in ex vivo organ culture system were exposed to adenoviruses. The wound areas were measured 36 h post injury. The results represent mean ± SD of at least 12 wounds and were analyzed by the Student's *t* test, relative to Ad β-Gal–infected tissues. ***$p < 0.001$, **$p < 0.01$, and *$p < 0.05$ are considered significant. C, no inhibitor; PD, PD98059, an inhibitor of ERK; SB, SB202190, an inhibitor of p38; and SP, SP600125, an inhibitor of JNK.

novirus-mediated MEKK1(WT) expression significantly accelerated wound closure; conversely, infecting wild-type mice wounds with Ad MEKK1 interfering RNA (iRNA) and Ad MEKK1(KM), expressing a kinase-inactive MEKK1, delayed the closure in comparison with uninfected, control Ad β-Gal-, or Ad GFP-infected wounds (Figure 1D).

Examination of the Ad β-Gal–infected wounds indicated that the infecting gene reached maximal expression in both dermis and epidermis at day 3 post infection (Figure 1E). Under these conditions, Ad MEKK1 iRNA suppressed MEKK1 expression by a factor of 3, reduced activity to one-half of control (Figure 1B), and caused an evident delay of wound healing at 4 d of infection (Figure 1D). In infected keratinocytes, Ad MEKK1 iRNA specifically reduced MEKK1 expression, which however was unaffected by a control adenovirus expressing IκBα iRNA (Supplemental Figure S1B). These data suggest that MEKK1 expression in skin epithelial cells and its activation by injury are required for optimal wound closure.

MEKK1 Activation Leads to Epithelial Cell Migration and Skin and Corneal Wound Reepithelialization

To further investigate epithelial cell functions affected by MEKK1, we performed an in vitro wound healing assay using primary mouse keratinocytes. Like its in vivo role in the full-thickness skin wounds of the wild-type mice described above, Ad MEKK1(WT) infection strongly accelerated keratinocyte wound healing. Neither Ad MEKK1(KM) nor Ad β-Gal had an effect on keratinocyte wound closure. Because Ad MEKK1(WT) infection did not alter cell proliferation rate (Supplemental Figure S1C), we conclude

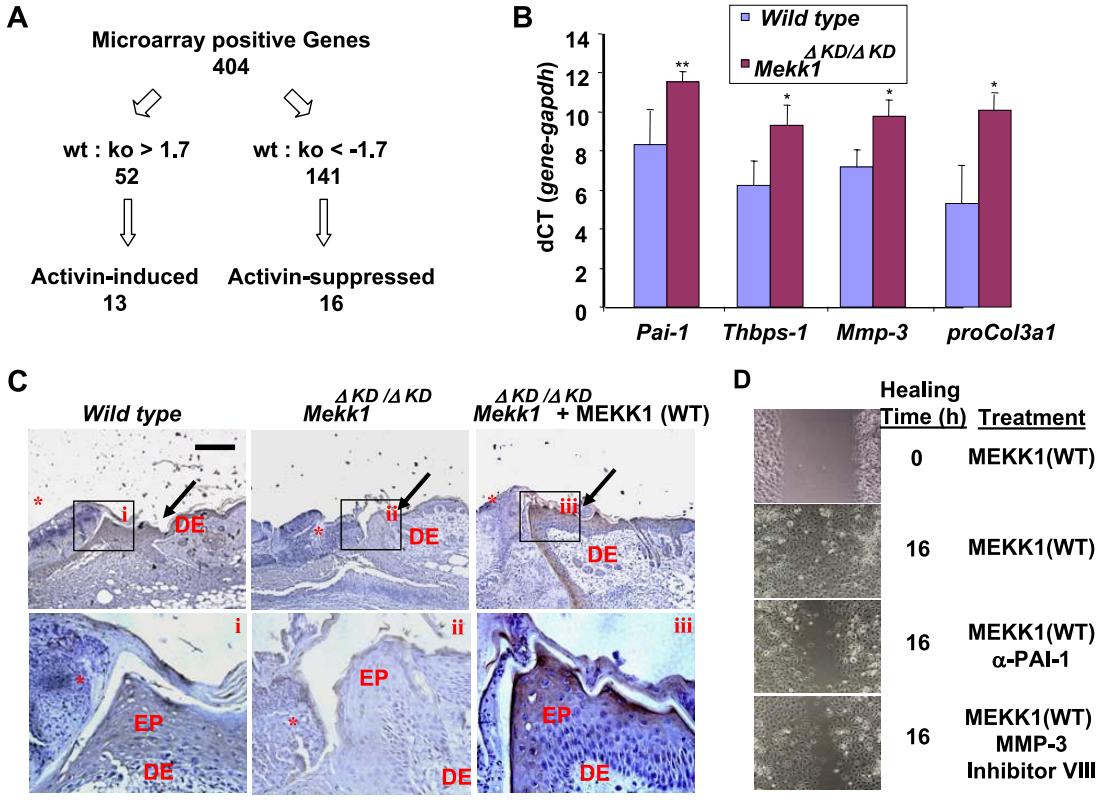

Figure 4. The induction of PAI-1 in the wound epidermis is dependent on MEKK1. (A) Summary of the microarray data. Of the MEKK1-dependent genes, 13 were induced and 16 suppressed by activin B treatment. Cultured epidermal keratinocytes were deprived of growth factors for 24 h, followed by exposure to 5 ng/ml activin B for 12 h or at the indicated times. (B) RNA isolated from epidermal keratinocytes of wild-type and *Mekk1*$^{\Delta KD/\Delta KD}$ mice were analyzed by real-time PCR for *Pai-1*, *Thbps-1*, *Mmp-3*, *Procol3a1*, and *Gapdh*. (C) Full-thickness skin wounds at days 1, 3, 5, and 7 were subjected to immunohistochemistry using anti-PAI-1. Increased PAI-1, characterized as diffused staining in brown color, was observed in the epidermis of the wounds of wild-type mice (i) or in *Mekk1*$^{\Delta KD/\Delta KD}$ infected by Ad MEKK1(WT) (iii), but it was almost undetectable in that of the *Mekk1*$^{\Delta KD/\Delta KD}$ (ii). Pictures were taken on skin tissues at day 5 of wounding, although similar PAI-1 expression pattern was observed in tissues at other wounding days. Bar, 250 μm. DE, dermis; EP, epidermis; *, exudates; and arrows, wounding edge. (D) In vitro wound healing assay of Ad MEKK1(WT)-infected HaCAT human keratinocytes with or without treatment with 5 μg/ml anti-PAI-1 and 10 μM MMP-3 inhibitor VIII before the wounding. Pictures were taken at 0 and 16 h.

that it promotes wound healing by stimulating keratinocyte migration.

The migration of wounding edge keratinocyte over ECMs, a process known as reepithelialization, is important for the closure of an epithelial wound. To study the role of MEKK1 in reepithelialization in vivo, we used a corneal epithelium debridement model, the healing of which is determined mainly by epithelial cell activities. When Ad β-Gal was used as eyedrops on in vivo corneal epithelial debridements, the β-Gal–positive cells accumulated at the wounding edge epithelium by 24 h post infection (Figure 2A). Exposure of the injured cornea to eyedrops containing Ad MEKK1(WT) significantly enhanced wound closure compared with Ad β-Gal, whereas Ad MEKK1(KM) delayed it (Figure 2B).

To further exclude the involvement of other cell types, such as infiltrated neutrophils and monocytes, we carried out an ex vivo organ culture, in which eyes isolated from mice were maintained in growth media. Infection of corneal debridements with Ad MEKK1(WT) caused a marked decrease of the wound to 5% of its original size, in contrast to 65% in infection with Ad β-Gal and >75% unhealed wound with Ad MEKK1(KM) (Figure 2C). As was the case in keratinocytes, the decrease in wound size by MEKK1(WT) was not due to induction of cell proliferation (Supplemental Figure S1D), further supporting a role for MEKK1 in stimulating epithelial cell migration and subsequent wound reepithelialization.

MEKK1-mediated JNK Activation Is Essential for Epithelial Cell Migration and Wound Healing

To identify signaling events downstream of MEKK1, we examined MAP kinase phosphorylation in the skin wounds. There was no obvious induction of MAPK phosphorylation in the wounded dermis, but a marked increase in the phosphorylation of JNKs and extracellular signal-regulated kinases (ERKs) (Figure 3B), and very little, if any, of p38 (our unpublished data), in the wounded epidermis. Although the phosphorylation of ERK remained at the same level in wild-type and *Mekk1*$^{\Delta KD/\Delta KD}$ mice, the phosphorylation of JNK was depended on MEKK1 and was reduced almost to basal levels in the wounds of the *Mekk1*$^{\Delta KD/\Delta KD}$ mice (Figure 3B).

We then investigated whether MAPK activity was necessary for MEKK1-induced wound healing. In vitro, adenoviral-mediated expression of MEKK1(WT) induced keratinocyte wound closure. Induction was abolished by the JNK inhibitor SP600125 and was partially delayed by ERK and p38 inhibitors (Figure 3C and Supplemental Figures S1E and S1F). Ex vivo, inclusion of the JNK inhibitor in the organ culture media prevented MEKK1(WT)-induced healing of corneal epithelial debridements almost completely, whereas

Table 2. Activin B and MEKK1-suppressed genes

Classification	Clone	Name	C wt:ko	A wt:ko	ko A:C	wt A:C
Receptor	AK017959	RIKEN cDNA 5830431115 gene	−3.29[a]	−5.13	−1.11	−1.72
Cell signaling	AJ272045	Calcium channel, voltage-dependent, γ subunit 4	−3.65	−6.51	1.02	−1.75
	M32502	Wingless-related MMTV integration site 3	−1.78	−2.86	−1.10	−1.77
	AF291489	Mus musculus vomeronasal receptor V1RB1 (V1rb1) gene	−2.19	−5.00	1.22	−1.88
	BC005584	Toll-interleukin 1 receptor (TIR) domain-containing adaptor protein	−3.45	−9.22	1.24	−2.15
	AK008851	Prostate stem cell antigen	−3.92	−7.68	−1.11	−2.18
Endocytosis	AK009469	RIKEN cDNA 2310022G12 gene	−1.93	−3.29	−1.01	−1.71
	NM_007469	Apolipoprotein C-1	−2.10	−3.12	−1.17	−1.74
	AF024519	Glucocorticoid-induced leucine zipper	−1.74	−3.06	−1.00	−1.77
Epithelial differentiation	NM_027137	Small proline rich-like 7	−2.66	−5.90	1.19	−1.87
	AJ005566	Small praline-rich protein 2H	−3.22	−8.07	1.02	−2.47
Unkown	NM_026543	RIKEN cDNA 3010026O09 gene	−1.90	−3.23	−1.01	−1.71
	NM_029667	RIKEN cDNA 2310069N01 gene	−2.87	−6.60	1.30	−1.76
	NM_026415	RIKEN cDNA 2310002J15 gene	−2.61	−4.60	−1.04	−1.84
	NM_026522	RIKEN cDNA 3110023E09 gene	−2.41	−4.44	−1.04	−1.92
	NM_025413	RIKEN cDNA 1110058A15 gene	−3.74	−10.27	1.01	−2.73

A, activin B; C, control; ko, keratinocytes from MEKK1-deficient mice; and wt, keratinocytes from wild-type mice.
[a] The numbers are -fold differences.

ERK and p38 inhibitors reduced healing by ~15% (Figure 2C). Conversely, specific activation of the JNK and p38 by the active MKK7 and MKK6, respectively (Liang *et al*., 2001), promoted the in vitro keratinocyte wound healing; Ad MKK7 infection pronouncedly enhanced the closure of in vivo full-thickness skin wounds and ex vivo corneal debridements (Figure 3, C–E). Hence, the MEKK1 signals are mediated mainly through JNK, the activation of which is sufficient for potentiation of wound reepithelialization.

The MEKK1 Pathway Leads to ECM Remodeling of Gene Expression

Because the JNKs are known to regulate transcription factors and to modulate gene expression, we believe that at least some of the MEKK1 effects on reepithelialization are the result of alteration of gene expression. To search for genes regulated by the MEKK1 pathway, we analyzed global gene expression patterns in primary mouse keratinocytes isolated from wild-type and *Mekk1*$^{\Delta KD/\Delta KD}$ mice. Of the 13,439 genes present on the arrays, 404 showed positive hybridization signals. The presence of a functional MEKK1 resulted in up-regulation of 52 genes and down-regulation of 141 (Figure 4A). Of 29 MEKK1 target genes, 13 were induced and 16 repressed by activin B, the wound-activated growth factor (Hubner *et al*., 1996) (Figure 4A and Tables 1 and 2).

The 16 genes repressed by the activin–MEKK1 pathway were classified into three major functional groups, including receptor and cell signaling, endocytosis, and epithelial cell differentiation, yet their gene products had no obvious connection to epithelial wound healing (Table 2). The 13 genes induced by the activin-MEKK1 pathway were grouped into four categories (Table 1) and detailed analyses revealed a functional relationship for 11 of them in the regulation of ECM homeostasis, resulting in increased expression of ECM components and the induction of proteases and their inhibitors that might further regulate ECM degradation (Albo *et al*., 1999; Chen *et al*., 2001a; Dallas *et al*., 2002). Interestingly, all these genes are known to be highly induced by tissue injury, and their expression is implicated in cell motility and wound healing (Chiquet-Ehrismann, 1995; Li *et al*., 2000; Engers *et al*., 2001; Uno *et al*., 2004).

We further studied the expression of several genes shown in the microarray data to be the most affected by the activin B–MEKK1 pathway (Table 1). Exposure of mouse keratinocytes to activin B strongly induced the expression of *Pai-1*, *Thbps-1*, *Mmp-3*, and *Procol3a1* at mRNA levels, an induction dependent on the presence of a functional MEKK1 (Figure 4B). Furthermore, skin injury resulted in an increase in PAI-1 expression in epidermis that was significant at day 1 and persisted until at least day 7 after wounding (Figure 4C; our unpublished data). PAI-1 induction was completely blocked by MEKK1 ablation, but it was restored by the expression of MEKK1(WT) using adenoviral-mediated gene delivery to the wounds (Figure 4C). It is interesting to note that the wound-induced PAI-1 was restricted to the epidermis, where MEKK1-dependent JNK phosphorylation was also detected. These results suggest a possible mechanism through which MEKK1 regulates gene expression and ECM homeostasis in the wound epithelium. Blocking the functions of these gene products, i.e., PAI-1 and MMP-3, by a neutralizing antibody or a chemical inhibitor caused a partial delay of MEKK1-stimulated epithelial cell migration and in vitro wound closure (Figure 4D).

MEKK1 Promotes Wounding Edge Epithelium Restoration

During injury repair, the ECM proteins provide an acellular scaffold for epithelial cell attachment and cell–cell interactions (Dawson *et al*., 1996). Microscopic examination of the wounded skin tissues showed that skin injury caused an increase of intercellular spaces in the basal layer epithelial cells. These morphological changes were transient in wild-type mice, prominent only at early (days 1–3) and less so at late (days 6–10) stages of the healing process (Figure 5A). At late stages, the epithelial cells resumed the adhesion structures (AD), resulting in tight cell–cell interaction and no intercellular spaces, similar to those in unwounded skin (Figure 5B). In contrast, the epidermis of the *Mekk1*$^{\Delta KD/\Delta KD}$ mice exhibited persistent large intercellular spaces (IS) between basal keratinocytes and loose cell–cell interactions even at late stages of injury. Apparently, MEKK1 facilitates the restoration of normal epithelial structure at the late stage of the injury repair.

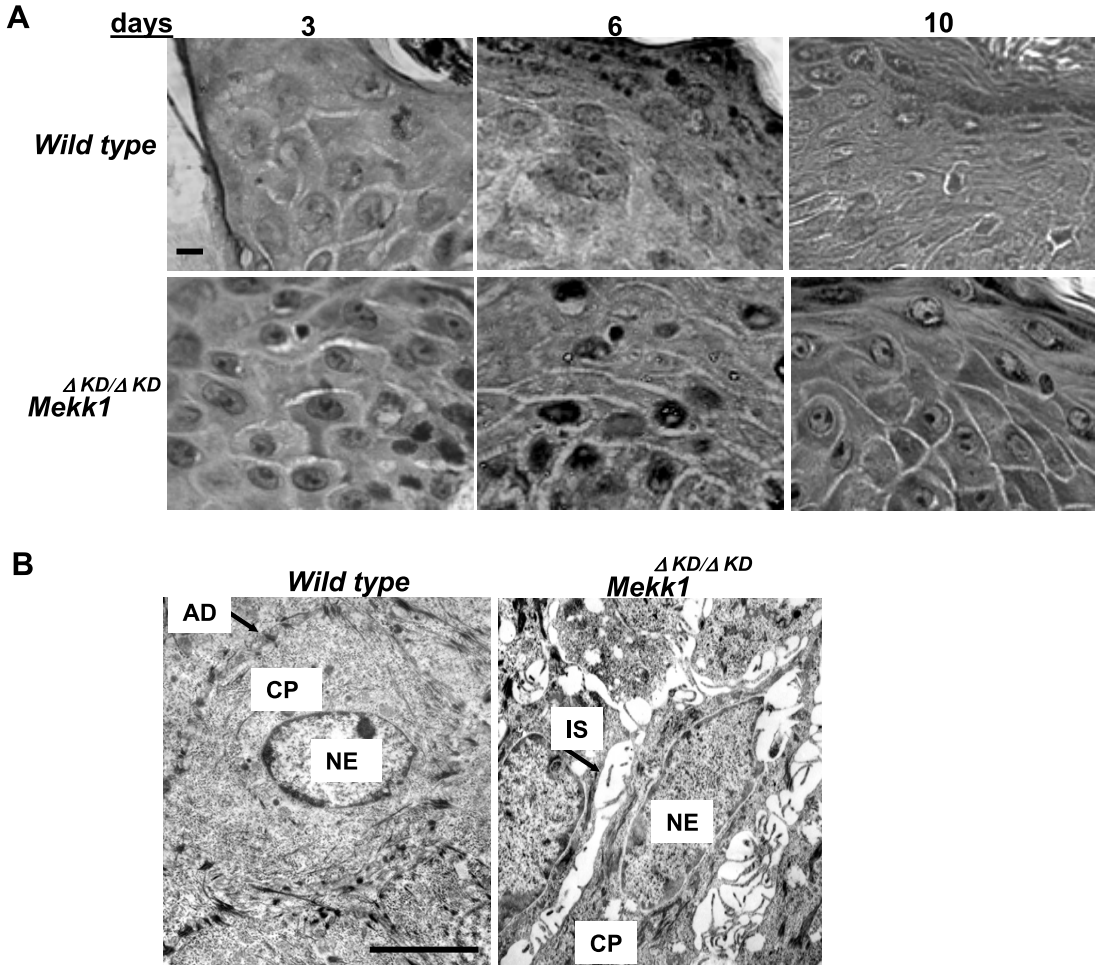

Figure 5. Lack of cell–cell junction formation in the wound epidermis of *Mekk1*$^{\Delta KD/\Delta KD}$ mice at late stage of healing. Morphological examination of the wounding edge epidermis at various days after injury. The wound tissues were examined under either phase-contrast microscopy (A) after H&E staining, and pictures were taken at 1000× magnification (bar, 10 μm), or electron microscopy (B), which was done on day 6 wounds. At early stage (day 3), both wild-type and *Mekk1*$^{\Delta KD/\Delta KD}$ mice show an apparent increase in intercellular spaces in the wounding edge epithelium. At late stage (days 6 and 10), only the *Mekk1*$^{\Delta KD/\Delta KD}$ mice display the spaces, whereas wild-type mice show tight cell–cell contact and the formation of desmosomes, similar to those present in normal unwounded skin. CP, cytoplasm; NE, nucleus. Bar, 10 μm.

DISCUSSION

In this report, we provide strong genetic evidence for a role of MEKK1 in wound reepithelialization and closure. We show that MEKK1 is abundantly expressed in the basal layer epithelial cells and that skin injury further induces MEKK1 expression and activity. MEKK1 ablation in mice by gene knockout or its down-regulation by iRNA causes delayed closure of full-thickness skin wounds; similarly, expression of kinase-inactive MEKK1 in wild-type mouse skin wounds reduces the healing rate. During tissue development, MEKK1 is known to be important for transmitting the activin B signals that lead to epithelial cell migration and eyelid morphogenesis (Zhang *et al*., 2003). In adult skin, activin B expression remains at a rather low level, but it is largely induced by skin injury in the hyperproliferative epithelium at the wound edge and in the migrating epithelial tongue (Hubner *et al*., 1996). We propose that adult skin injury reactivates the developmental activin–MEKK1 pathway and that this pathway activation leads to morphological changes of the wounding edge epithelium required for reepithelialization.

In the wounding edge epithelial cells, MEKK1 activity leads to the induction of JNK, but the induction of ERK MAPKs is independent of MEKK1. The involvement of JNK in wound healing has mostly been established in *Drosophila*, in which DJNK regulates the healing of imaginal disk and adult epithelial wounds (Ramet *et al*., 2002; Bosch *et al*., 2005). We show that JNK activities are essential for mediating MEKK1-induced epithelial cell migration and corneal wound reepithelialization. This is the first identification of a mammalian pathway in which MEKK1 acts as the specific MAPK kinase kinase for JNK activation, leading to epithelial wound healing. Activation of JNK is not only essential but also sufficient in stimulating keratinocyte migration and epithelial wound closure in mammals, similar to its ancestral role in *Drosophila*.

Activation of the activin B pathway leads to the induction, among others, of the *Pai-1* gene, whose promoter contains an activator protein-1 binding site required for *Pai-1* transcriptional activation (Keeton *et al*., 1991). PAI-1 induction depends on MEKK1, as shown by its marked decrease in the *Mekk1*-null cells and epidermal wounds; however, decrease

of PAI-1 expression alone does not fully explain delayed wound closure in MEKK1-null mice, because PAI-1 ablation in mice does not result in defective healing of skin wounds (Chan *et al*., 2001). Expression of several genes involved in ECM remodeling, such as tissue inhibitor of metalloproteinase-1, tenascin C, thrombospondin 1, and procollagens III and IV, all known to have a role in the control of cell motility and wound healing (Chiquet-Ehrismann, 1995; Roth *et al*., 1999; Li *et al*., 2000; Engers *et al*., 2001; Uno *et al*., 2004; Koivukangas *et al*., 2005), are also regulated by the activin B–MEKK1 pathway, as shown by our global gene profiling studies. In all likelihood, the role of the MEKK1 pathway in wound healing requires the activation of a more extensive group of genes, because neither blocking PAI-1 function with a neutralizing antibody nor blocking MMP-3 with a chemical inhibitor results in the complete inhibition of MEKK1-stimulated epithelial cell migration. Detailed analyses of the functional relationships of MEKK1-dependent genes provide converging evidence for the role of this kinase in orchestrating ECM accumulation, which may ensure epithelial cell adhesion to matrix to promote successful migration and wound healing (Madlener, 1998; Providence and Higgins, 2004). Indeed, the epithelial cells in wild-type wounds form tight cell–cell interactions and restore normal epithelium architecture at day 6 of injury, whereas those in $Mekk1^{\Delta KD/\Delta KD}$ wounds fail to do so. Hence, regulation of gene expression and ECM accumulation and remodeling are a major consequence of the wound-induced MEKK1 activation.

Adenoviruses deliver genes to the desired target tissues in the corneal epithelium wounds; however, they may cause minor inflammatory cell infiltration, such that the effect of Ad MEKK1(WT) on wound healing in vivo may be less pronounced than its effect in ex vivo organ culture. In the full-thickness skin wounds, local injection of adenoviruses delivers genes to both dermis and epidermis. Although MEKK1 expression in the dermis does not seem to have serious effects on the wound healing capability, it is still desirable to explore other gene delivery vehicles or application methods for MEKK1 to achieve an optimal tissue-specific outcome.

The expression of the endogenous MEKK1 is restricted to the epithelium of the skin, in which tissue MEKK1 is specifically required for JNK activation and PAI-1 expression after skin injury. Correspondingly, overexpression of a kinase active MEKK1(WT) accelerates the healing of skin and corneal epithelium wounds. In this case, MEKK1 activation leads to the migration, but not the proliferation, of epithelial cells, and it also leads to ECM accumulation in epithelium, but not in dermis, which is usually responsible for scar tissue formation (Setoguchi *et al*., 1994). No single signaling pathway activation can fully replace the complex signaling processes of wound healing, but the activation of MEKK1 seems to be responsible, at least partly, for the specific process of reepithelialization by controlling epithelial cell migration. Such cell type and functional specificity exhibited by MEKK1 warrants its use as a promising therapeutic strategy to accelerate wound reepithelialization. That a transient MEKK1 expression is all that is necessary to enhance wound closure points at the possibility of using MEKK1 activation to improve the healing of wounds that require clinical attention, such as those in corneal injuries, severe burns, chronic skin ulcers, or diabetes (Setoguchi *et al*., 1994).

ACKNOWLEDGMENTS

We thank Alvaro Puga for a critical reading of the manuscript, Susanne Wells for providing pAdtrack vector and helping with adenoviral preparation techniques, Christine Kane for teaching us the full-thickness skin wounding assay, Esmond Geh for providing purified anti-MEKK1, and Stacey Andringa for processing electron microscopy samples. The work is supported by National Institutes of Health Grants R01 EY15227, EY13755, and P30 ES06096, and Research to Prevent Blindness (New York, NY).

REFERENCES

Albo, D., Berger, D. H., Vogel, J., and Tuszynski, G. P. (1999). Thrombospondin-1 and transforming growth factor beta-1 upregulate plasminogen activator inhibitor type 1 in pancreatic cancer. J. Gastrointest. Surg. *3*, 411–417.

Ashcroft, G. S., *et al*. (1999). Mice lacking Smad3 show accelerated wound healing and an impaired local inflammatory response. Nat. Cell Biol. *1*, 260–266.

Bamberger, C., Scharer, A., Antsiferova, M., Tychsen, B., Pankow, S., Muller, M., Rulicke, T., Paus, R., and Werner, S. (2005). Activin controls skin morphogenesis and wound repair predominantly via stromal cells and in a concentration-dependent manner via keratinocytes. Am. J. Pathol. *167*, 733–747.

Bosch, M., Serras, F., Martin-Blanco, E., and Baguna, J. (2005). JNK signaling pathway required for wound healing in regenerating Drosophila wing imaginal discs. Dev. Biol. *280*, 73–86.

Chan, J. C., Duszczyszyn, D. A., Castellino, F. J., and Ploplis, V. A. (2001). Accelerated skin wound healing in plasminogen activator inhibitor-1-deficient mice. Am. J. Pathol. *159*, 1681–1688.

Chen, C. C., Mo, F. E., and Lau, L. F. (2001a). The angiogenic factor Cyr61 activates a genetic program for wound healing in human skin fibroblasts. J. Biol. Chem. *276*, 47329–47337.

Chen, N., Nomura, M., She, Q. B., Ma, W. Y., Bode, A. M., Wang, L., Flavell, R. A., and Dong, Z. (2001b). Suppression of skin tumorigenesis in c-Jun NH(2)-terminal kinase-2-deficient mice. Cancer Res. *61*, 3908–3912.

Chiquet-Ehrismann, R. (1995). Tenascins, a growing family of extracellular matrix proteins. Experientia *51*, 853–862.

Dallas, S. L., Rosser, J. L., Mundy, G. R., and Bonewald, L. F. (2002). Proteolysis of latent transforming growth factor-beta (TGF-beta)-binding protein-1 by osteoclasts. A cellular mechanism for release of TGF-beta from bone matrix. J. Biol. Chem. *277*, 21352–21360.

Dawson, R. A., Goberdhan, N. J., Freedlander, E., and MacNeil, S. (1996). Influence of extracellular matrix proteins on human keratinocyte attachment, proliferation and transfer to a dermal wound model. Burns *22*, 93–100.

Dudoit, S., and Fridlyand, J. (2002). A prediction-based resampling method for estimating the number of clusters in a dataset. Genome Biol. *3*, RESEARCH0036.

Engers, R., Springer, E., Michiels, F., Collard, J. G., and Gabbert, H. E. (2001). Rac affects invasion of human renal cell carcinomas by up-regulating tissue inhibitor of metalloproteinases (TIMP)-1 and TIMP-2 expression. J. Biol. Chem. *276*, 41889–41897.

Feijen, A., Goumans, M. J., and van den Eijnden-van Raaij, A. J. (1994). Expression of activin subunits, activin receptors and follistatin in postimplantation mouse embryos suggests specific developmental functions for different activins. Development *120*, 3621–3637.

Henkemeyer, M., Orioli, D., Henderson, J. T., Saxton, T. M., Roder, J., Pawson, T., and Klein, R. (1996). Nuk controls pathfinding of commissural axons in the mammalian central nervous system. Cell *86*, 35–46.

Hibi, M., Lin, A., Smeal, T., Minden, A., and Karin, M. (1993). Identification of an oncoprotein- and UV-responsive protein kinase that binds and potentiates the c-Jun activation domain. Genes Dev. *7*, 2135–2148.

Hubner, G., Hu, Q., Smola, H., and Werner, S. (1996). Strong induction of activin expression after injury suggests an important role of activin in wound repair. Dev. Biol. *173*, 490–498.

Keeton, M. R., Curriden, S. A., van Zonneveld, A. J., and Loskutoff, D. J. (1991). Identification of regulatory sequences in the type 1 plasminogen activator inhibitor gene responsive to transforming growth factor beta. J. Biol. Chem. *266*, 23048–23052.

Koivukangas, V., Oikarinen, A., Risteli, J., Haukipuro, K. (2005). Effect of jaundice and its resolution on wound re-epithelization, skin collagen synthesis, and serum collagen propeptide levels in patients with neoplastic pancreaticobiliary obstruction. J. Surg. Res. *124*, 237–243.

Li, F., Goncalves, J., Faughnan, K., Steiner, M. G., Pagan-Charry, I., Esposito, D., Chin, B., Providence, K. M., Higgins, P. J., and Staiano-Coico, L. (2000). Targeted inhibition of wound-induced PAI-1 expression alters migration and differentiation in human epidermal keratinocytes. Exp. Cell Res. *258*, 245–253.

Liang, Q., Wiese, R. J., Bueno, O. F., Dai, Y. S., Markham, B. E., and Molkentin, J. D. (2001). The transcription factor gata4 is activated by extracellular signal-regulated kinase 1- and 2-mediated phosphorylation of serine 105 in cardiomyocytes. Mol. Cell. Biol. *21*, 7460–7469.

Liu, C. Y., Zhu, G., Westerhausen-Larson, A., Converse, R., Kao, C. W., Sun, T. T., and Kao, W. W. (1993). Cornea-specific expression of K12 keratin during mouse development. Curr. Eye Res. *12*, 963–974.

Madlener, M. (1998). Differential expression of matrix metalloproteinases and their physiological inhibitors in acute murine skin wounds. Arch. Dermatol. Res. 290 (Suppl.) S24–S29.

Providence, K. M., and Higgins, P. J. (2004). PAI-1 expression is required for epithelial cell migration in two distinct phases of in vitro wound repair. J. Cell Physiol. *200*, 297–308.

Ramet, M., Lanot, R., Zachary, D., and Manfruelli, P. (2002). JNK signaling pathway is required for efficient wound healing in *Drosophila*. Dev. Biol. *241*, 145–156.

Reiner, A., Yekutieli, D., and Benjamini, Y. (2003). Identifying differentially expressed genes using false discovery rate controlling procedures. Bioinformatics *19*, 368–375.

Roth, J. J., Sung, J. J., Granick, M. S., Solomon, M. P., Longaker, M. T., Rothman, V. L., Nicosia, R. F., and Tuszynski, G. P. (1999). Thrombospondin 1 and its specific cysteine-serine-valine-threonine-cysteine-clycine receptor in fetal wounds. Ann. Plast. Surg. *42*, 553–563.

Rouabhia, M., Germain, L., Belanger, F., Guignard, R., and Auger, F. A. (1992). Optimization of murine keratinocyte culture for the production of graftable epidermal sheets. J. Dermatol. *19*, 325–334.

Schlesinger, T. K., Fanger, G. R., Yujiri, T., and Johnson, G. L. (1998). The TAO of MEKK. Front. Biosci. *3*, 1181–1186.

Schrewe, H., Gendron-Maguire, M., Harbison, M. L., and Gridley, T. (1994). Mice homozygous for a null mutation of activin beta B are viable and fertile. Mech. Dev. *47*, 43–51.

Setoguchi, Y., Jaffe, H. A., Danel, C., and Crystal, R. G. (1994). Ex vivo and in vivo gene transfer to the skin using replication-deficient recombinant adenovirus vectors. J. Investig. Dermatol. *102*, 415–421.

Uno, K., Hayashi, H., Kuroki, M., Uchida, H., Yamauchi, Y., Kuroki, M., and Oshima, K. (2004). Thrombospondin-1 accelerates wound healing of corneal epithelia. Biochem. Biophys. Res. Commun. *315*, 928–934.

Vassalli, A., Matzuk, M. M., Gardner, H. A., Lee, K. F., and Jaenisch, R. (1994). Activin/inhibin beta B subunit gene disruption leads to defects in eyelid development and female reproduction. Genes Dev. *8*, 414–427.

Wankell, M., Munz, B., Hubner, G., Hans, W., Wolf, E., Goppelt, A., and Werner, S. (2001). Impaired wound healing in transgenic mice overexpressing the activin antagonist follistatin in the epidermis. EMBO J. *20*, 5361–5372.

Werner, S., and Grose, R. (2003). Regulation of wound healing by growth factors and cytokines. Physiol. Rev. *83*, 835–870.

Wolfinger, R. D., Gibson, G., Wolfinger, E. D., Bennett, L., Hamadeh, H., Bushel, P., Afshari, C., and Paules, R. S. (2001). Assessing gene significance from cDNA microarray expression data via mixed models. J. Comput. Biol. *8*, 625–637.

Xia, Y., Makris, C., Su, B., Li, E., Yang, J., Nemerow, G. R., and Karin, M. (2000). MEK kinase 1 is critically required for c-Jun N-terminal kinase activation by proinflammatory stimuli and growth factor-induced cell migration. Proc. Natl. Acad. Sci. USA *97*, 5243–5248.

Xia, Y., Wu, Z., Su, B., Murray, B., and Karin, M. (1998). JNKK1 organizes a MAP kinase module through specific and sequential interactions with upstream and downstream components mediated by its amino-terminal extension. Genes Dev. *12*, 3369–3381.

Yujiri, T., Ware, M., Widmann, C., Oyer, R., Russell, D., Chan, E., Zaitsu, Y., Clarke, P., Tyler, K., Oka, Y., et al. (2000). MEK kinase 1 gene disruption alters cell migration and c-Jun NH2-terminal kinase regulation but does not cause a measurable defect in NF-kappa B activation. Proc. Natl. Acad. Sci. USA *97*, 7272–7277.

Zhang, L., Deng, M., Parthasarathy, R., Wang, L., Mongan, M., Molkentin, J. D., Zheng, Y., and Xia, Y. (2005). MEKK1 transduces activin signals in keratinocytes to induce actin stress fiber formation and migration. Mol. Cell Biol. *25*, 60–65.

Zhang, L., Wang, W., Hayashi, Y., Jester, J. V., Birk, D. E., Gao, M., Liu, C. Y., Kao, W. W., Karin, M., and Xia, Y. (2003). A role for MEK kinase 1 in TGF-beta/activin-induced epithelium movement and embryonic eyelid closure. EMBO J. *22*, 4443–4454.